Since January 2020 Elsevier has created a COVID-19 resource centre with free information in English and Mandarin on the novel coronavirus COVID-19. The COVID-19 resource centre is hosted on Elsevier Connect, the company's public news and information website.

Fish and Shellfish Immunology 99 (2020) 99–106

Contents lists available at ScienceDirect

Fish and Shellfish Immunology

journal homepage: www.elsevier.com/locate/fsi

Full length article

Grass carp reovirus VP56 represses interferon production by degrading phosphorylated IRF7

Can Zhang[a,c], Long-Feng Lu[a], Zhuo-Cong Li[a,c], Xiao-Yu Zhou[a,c], Yu Zhou[a,c], Dan-Dan Chen[a], Shun Li[a,*], Yong-An Zhang[a,b,**]

[a] Institute of Hydrobiology, Chinese Academy of Sciences, Wuhan, China
[b] State Key Laboratory of Agricultural Microbiology, College of Fisheries, Huazhong Agricultural University, Wuhan, China
[c] University of Chinese Academy of Sciences, Beijing, China

ARTICLE INFO

Keywords:
VP56
GCRV
Immune evasion
IRF7
Interferon

ABSTRACT

Grass carp reovirus (GCRV) is an efficient pathogen causing high mortality in grass carp, meanwhile, fish interferon (IFN) is a powerful cytokine enabling host cells to establish an antiviral state; therefore, the strategies used by GCRV to escape the cellular IFN response need to be investigated. Here, we report that GCRV VP56 inhibits host IFN production by degrading the transcription factor IFN regulatory factor 7 (IRF7). First, overexpression of VP56 inhibited the IFN production induced by the polyinosinic-polycytidylic acid (poly I:C) and mitochondrial antiviral signaling protein (MAVS), while the capacity of IRF7 on IFN induction was unaffected. Second, VP56 interacted with RLRs but did not affect the stabilization of the proteins in the normal state, while the phosphorylated IRF7 activated by TBK1 was degraded by VP56 through K48-linked ubiquitination. Finally, overexpression of VP56 remarkably reduced the host cellular *ifn* transcription and facilitated viral proliferation. Taken together, our results demonstrate that GCRV VP56 suppresses the host IFN response by targeting phosphorylated IRF7 for ubiquitination and degradation.

1. Introduction

Grass carp reovirus (GCRV), which belongs to the genus *Aquareovirus* of the family *Reoviridae*, has caused severe epidemic outbreaks of hemorrhagic disease and has an extremely high mortality rate among grass carp (*Ctenopharyngodon idella*) [1]. At present, known GCRV strains can be divided into three distinct subtypes based on sequence comparisons and analysis. The representative strains of the three groups are GCRV-873 (GCRV-I), GCRV-HZ08 (GCRV-II), and GCRV-104 (GCRV-III) [2]. The most commonly isolated strain is GCRV-II [3]. GCRV is a double-stranded RNA (dsRNA) virus and the genome consists of 11 segments (termed s1–s11) encased in a multilayered icosahedral capsid shell [4,5]. The protein sequence comparison showed that the similarity among the three groups is < 20%, so the functions of the encoded proteins are likely diverse. For instance, s7 of GCRV-I has been found to encode a non-structural protein (NS16, NS31) [5,6]. S7 of both GCRV-II and GCRV-III are codified as a fiber like protein, which are predicted to be 56 KDa (VP56) and 55 KDa (VP55) [7,8]. In recent years, great progress has been made in the pathogenesis of GCRV and the host response to GCRV infection. For example, by using high-throughput methods such as transcriptomic and proteomic analyses, many immune-related genes have been identified as being involved in a GCRV infection [9]. Overexpression of Mxs blocks the replication of GCRV and delays the CPE induced by GCRV infection [10]. In *crucian carp*, viperin confers cells significant protection against GCRV infection [11].

Interferon (IFN) response plays an essential role in protecting the host against virus infection [12,13]. The host possesses conserved pathogen recognition receptors (PRRs) that can sense viral RNAs and trigger multiple intracellular signaling pathways, including the retinoic acid-inducible gene I (RIG-I)-like receptor (RLR) pathway, which eventually results in the production of IFN to set up the antiviral state [12,14–16]. The specific RLR pathway is as follows: upon binding with viral RNA, the N-terminal caspase recruiting domain (CARD) of the RLR family (including RIG-I and melanoma differentiation-associated gene 5 (MDA5), interacts with another CARD-containing protein, mitochondrial antiviral signaling protein (MAVS, also called VISA, IPS-1, and Cardif) [17–20]. Then, the signal transmits to the downstream mediator of IFN regulatory factor 3 (IRF3) activation (MITA, also known as STING, ERIS, or MYPS) and TANK binding kinase 1 (TBK1) [21].

* Corresponding author. Institute of Hydrobiology, Chinese Academy of Sciences, Wuhan, 430072, China.
** Corresponding author. College of Fisheries, Huazhong Agricultural University, Wuhan, 430070, China.
E-mail addresses: bob@ihb.ac.cn (S. Li), yonganzhang@mail.hzau.edu.cn (Y.-A. Zhang).

https://doi.org/10.1016/j.fsi.2020.02.004
Received 16 September 2019; Received in revised form 16 January 2020; Accepted 3 February 2020
Available online 04 February 2020
1050-4648/

Subsequently, activated TBK1 phosphorylates IRF3/7 are translocated to the nucleus and trigger the transcription of IFN [22,23]. Similar to mammals, fish also possess a conserved RLRs signaling pathway. For example, MAVS or MITA plays an important role in IFN activation in zebrafish (*Danio rerio*), which can significantly decrease the probability of viral infection [24,25]. Overexpression of grass carp TBK1 induces the expression of IRF7 and IFN-stimulated genes (ISGs), and inhibits the replication of GCRV [26]. IRF7 in zebrafish and grass carp also exhibits a critical role in IFN activation [27].

However, viruses have evolved a multitude of elaborate strategies to escape the host immune response. One such mechanism is to blunt IFN production. IRF7 is a key transcription factor that regulates IFN induction in response to viral infection [28,29], most signals ultimately converge on IRF7, so it is targeted by viruses as a major negative regulatory target to decrease the IFN response and facilitate viral replication. For instance, porcine reproductive and respiratory syndrome (PRRS) utilizes the nsp 7 protein to inhibit IRF7 expression, thereby down-regulating IFN production and counteracting the host antiviral state [30]. The $3C^{pro}$ of Seneca Valley Virus (SVV) reduces IRF3 and IRF7 protein expression and phosphorylation via its protease activity, thus blocking IFN transcription to escape the host immune response [31]. Kaposi's sarcoma-associated herpesvirus (KSHV)-encoded viral interferon regulatory factor 4 (vIRF4) interacts with IRF7, resulting in the inhibition of IRF7 dimerization and ultimately suppressing IFN production [32].

As a highly virulent pathogen that causes severe hemorrhagic disease and tremendous mortality in fish, GCRV likely has strategies to negatively regulate or evade the host immune response. In our previous study, the GCRV VP41 attenuated MITA phosphorylation by acting as a decoy substrate of TBK1, thus reducing IFN production and facilitating viral replication. To further investigate the immune evasion strategies of GCRV, we further revealed that GCRV VP56 is associated with IRF7 and promotes the K48-linked ubiquitination and degradation of IRF7, thereby inhibiting IFN expression and accelerating viral proliferation. These results will lay a foundation for further studying host-virus interactions among lower vertebrates.

2. Materials and methods

2.1. Cells and viruses

Human embryonic kidney (HEK) 293T cells were provided by Dr. Xing Liu (Institute of Hydrobiology, Chinese Academy of Sciences) and were grown at 37 °C in 5% CO_2 in Dulbecco's modified Eagle's medium (DMEM; Invitrogen) supplemented with 10% fetal bovine serum (FBS, Invitrogen). Epithelioma papulosum cyprini (EPC) cells and Grass carp ovary (GCO) cells were maintained at 28 °C in 5% CO_2 in medium 199 (Invitrogen) supplemented with 10% FBS. GCRV (strain 106, GCRV-II) was a gift from Lingbing Zeng (Yangtze River Fisheries Research Institute, Chinese Academy of Fishery Sciences). Because GCRV-II cannot cause a cytopathic effect (CPE) but can propagate in GCO cells, the cultured media with GCO cells infected with GCRV-II for 8 days were harvested and stored at −80 °C until used.

2.2. Plasmid construction and reagents

The open reading frame (ORF) of GCRV VP56 (KC201172.1) was generated by PCR and then cloned into pcDNA3.1 (+) (Invitrogen), pCMV-Myc (Clontech), or pCMV-HA vectors (Clontech), respectively. The ORFs of grass carp MAVS (KF366908.1), MITA (JN786909.1), TBK1 (JN704345.1), IRF3 (KT347289.1), and IRF7 (KY613780.1) were cloned using the vectors previously described [33] For subcellular localization, the ORF of VP56 was inserted into pEGFP-N3 vector (Clontech). The ORFs of MAVS, MITA, TBK1, IRF3, and IRF7 were also inserted into pCS2-mCherry vector (Clontech). The expression plasmids for Flag-DrTBK1, HA-DrIRF3, HA-DrIRF7, and Myc- DrIRF7 were described previously [33]. For promoter activity analysis, IFN1pro-Luc construct was generated by insertion of corresponding 5′-flanking regulatory region of IFN1 promoter (GU139255.1) into pGL3-basic luciferase reporter vector (Promega, Madison, WI). The ISRE-Luc plasmid in the pGL3-basic luciferase reporter vector (Promega) was constructed as described previously [34]. The Renilla luciferase internal control vector (pRL-TK) was purchased from Promega. The primers including the restriction enzyme cutting sites used for plasmid construction are listed in Supplemental Table I. All constructs were confirmed by DNA sequencing.

2.3. Luciferase activity assay

EPC cells were seeded into 24-well plates overnight and co-transfected with various constructs at a ratio of 10:10:1 (MAVS/IRF7, IFN1pro/ISRE-Luc, and pRL-TK expression vectors). The pRL-TK was used to normalize the expression levels of the transfected plasmids. An empty vector pcDNA3.1 (+) was used to maintain equivalent amounts of DNA in each well. The transfection of poly I: C was performed at 24 h after post-transfection, and cells were harvested at 24 h after poly I: C transfection. At 48 h post transfection, the cells were washed with phosphate-buffered saline (PBS) and lysed for measuring luciferase activity by a dual-luciferase reporter assay system, according to the manufacturer's instructions (Promega). The results are representative of more than three independent experiments, each performed in triplicate.

2.4. Transient transfection and virus infection

Transient transfections were performed in EPC cells seeded in 6-well or 24-well plates by using X-tremeGENE HP DNA Transfection Reagent (Roche) according to the manufacturer's protocol. For the antiviral assay using 24-well plates, EPC cells were transfected with 0.5 μg pcDNA3.1 (+)-VP56 or the empty vector. At 24 h post-transfection, cells were infected with SVCV at a multiplicity of infection (MOI = 0.001). After 2 or 3 d, supernatant aliquots were harvested for detection of virus titers, the cell monolayers were fixed by 4% paraformaldehyde (PFA) and stained with 1% crystal violet for visualizing CPE. For virus titration, 200 μl of culture medium were collected at 48 h post-infection, and used for plaque assay. The supernatants were subjected to 3-fold serial dilutions and then added (100 μl) onto a monolayer of EPC cells cultured in a 96-well plate. After 48 or 72 h, the medium was removed and the cells were washed with PBS, fixed by 4% PFA and stained with 1% crystal violet. The virus titer was expressed as 50% tissue culture infective dose ($TCID_{50}$/ml). Results are representative of three independent experiments.

2.5. RNA extraction, reverse transcription, and qPCR

Total RNAs were extracted using the Trizol reagent (Invitrogen). cDNA was synthesized using a GoScript reverse transcription system (Promega), according to the manufacturer's instructions. Quantitative real-time PCR (qPCR) was performed with Fast SYBR Green PCR Master Mix (Bio-Rad) on the CFX96 Real-Time System (Bio-Rad). PCR conditions were as follows: 95 °C for 5 min and then 40 cycles of 95 °C for 20 s, 60 °C for 20 s, and 72 °C for 20 s. The β-actin gene was used as an internal control. Primer sequences are listed in Supplemental Table I. The relative fold changes or relative mRNA of level were calculated by comparison to the corresponding controls using the $2^{-\Delta\Delta CT}$ method. Three independent experiments were conducted for statistical analysis.

2.6. Co-immunoprecipitation (co-IP) assay

In transient transfection and co-IP experiments, we used HEK 293T cells instead of EPC cells because of their high transfection efficiency. The HEK 293T cells seeded in 10-cm^2 dishes overnight were transfected with 5 μg Flag-MAVS/TBK1/MITA/IRF3/IRF7 and 5 μg Myc-VP56. At

24 h post transfection, the medium was removed carefully, and the cell monolayer was washed twice with 10 ml of ice-cold PBS. Then the cells were lysed in 1 ml of radioimmunoprecipitation lysis buffer (1% Nonidet P-40, 50 mM Tris-HCl, pH 7.5, 150 mM NaCl, 1 mM EDTA, 1 mM NaF, 1 mM sodium orthovanadate [Na_3VO_4], 1 mM PMSF, 0.25% sodium deoxycholate) containing protease inhibitor mixture (Sigma-Aldrich) at 4 ˚C for 1 h on a rocker platform. The cellular debris was removed by centrifugation at 12,000 × *g* for 15 min at 4 ˚C. The supernatant was transferred to a fresh tube and incubated with 30 μl of anti-hemagglutinin (HA)-agarose beads or anti-Flag affinity gel (Sigma-Aldrich) overnight at 4 ˚C with constant agitation. These samples were further analyzed by immunoblotting. Immunoprecipitated proteins were collected by centrifugation at 5,000 × *g* for 1 min at 4 ˚C, washed three times with lysis buffer, and resuspended in 50 μl of 2 × SDS sample buffer. The immunoprecipitates and whole-cell lysates (WCLs) were analyzed by IB with the indicated Abs.

2.7. In vivo ubiquitination assay

The cells were lysed using a RIPA lysis buffer containing 1% SDS and denatured by heating for 10 min. The supernatants were diluted with lysis buffer until the concentration of SDS was decreased to 0.1%. The diluted supernatants were incubated with 20 μl anti-Myc affinity gel (Sigma-Aldrich) overnight at 4 ˚C with constant agitation. These samples were further analyzed by immunoblotting (IB). Immunoprecipitated proteins were collected by centrifugation at 5000 × *g* for 1 min at 4 ˚C, washed three times with lysis buffer and resuspended in 50 μl 2 × SDS sample buffer.

2.8. Immunoblot analysis

Immunoprecipitates or WCLs were separated by 10% SDS-PAGE and transferred to polyvinylidene difluoride (PVDF) membrane (Bio-Rad). The membranes were blocked for 1 h at room temperature in TBST buffer (25 mM Tris- HCl, 150 mM NaCl, 0.1% Tween 20, pH 7.5) containing 5% nonfat dry milk, probed with the primary Abs indicated on the figures at an appropriate dilution overnight at 4 ˚C, washed three times with TBST, and then incubated with secondary Abs for 1 h at room temperature. After three additional washes with TBST, the membranes were stained with the Immobilon Western chemiluminescent horseradish peroxidase (HRP) substrate (Millipore) and detected by using an Image Quant LAS 4000 system (GE Healthcare). Abs were diluted as follows: anti-β-actin (Cell Signaling Technology) at 1:1,000, anti-Flag/HA (Sigma-Aldrich) at 1:3,000, anti-Myc (Santa Cruz Biotechnology) at 1:3,000, and HRP-conjugated anti-rabbit IgG or anti-mouse IgG (Thermo Scientific) at 1:5,000. Results are representative of data from three independent experiments.

2.9. In vitro protein dephosphorylation assay

Transfected HEK 293T cells were lysed as described above, except that the phosphatase inhibitors (Na_3VO_4 and EDTA) were omitted from the lysis buffer. Protein dephosphorylation was carried out in 100 μl reaction mixtures consisting of 100 μg of cell protein and 10 U of CIP (Sigma-Aldrich). The reaction mixtures were incubated at 37 ˚C for 40 min, followed by immunoblot analysis.

2.10. Fluorescence microscopy

EPC cells were plated onto coverslips in six-well plates and transfected with the indicated plasmids for 24 h. Then the cells were washed twice with PBS and fixed with 4% paraformaldehyde (PFA) for 1 h. After being washed three times with PBS, the cells were stained with 4′, 6-diamidino-2-phenylindole (DAPI) (1 μg/ml; Beyotime) for 8 min in the dark at room temperature. Finally, the coverslips were washed and observed with a confocal microscope under a × 63 oil immersion objective (SP8; Leica).

2.11. Statistics analysis

Luciferase and qPCR assay data are expressed as the mean ± standard error of the mean (SEM). Error bars indicate the SEM ($n = 3$, biologically independent samples). The p values were calculated by one-way analysis of variance (ANOVA) with Dunnett's post hoc test (SPSS Statistics, version 19; IBM). A p value < 0.05 was considered statistically significant.

3. Results

3.1. GCRV VP56 inhibits poly I:C-induced IFN expression

Previously, our study has demonstrated that GCRV VP41 reduces MITA phosphorylation and blocks IFN production, thus escaping the host immune response. Given that one virus should possess multiple strategies to elude host defense mechanisms, other immune escape mechanisms of GCRV should be identified. Here, to further investigate the other strategies used by GCRV to combat the host, other constructs of GCRV segments were employed for luciferase experiments *in vitro*, and the s7-encoded protein (VP56) exhibited the potential to inhibit host IFN activation. Upon infection with GCRV, the viral s7 gene was

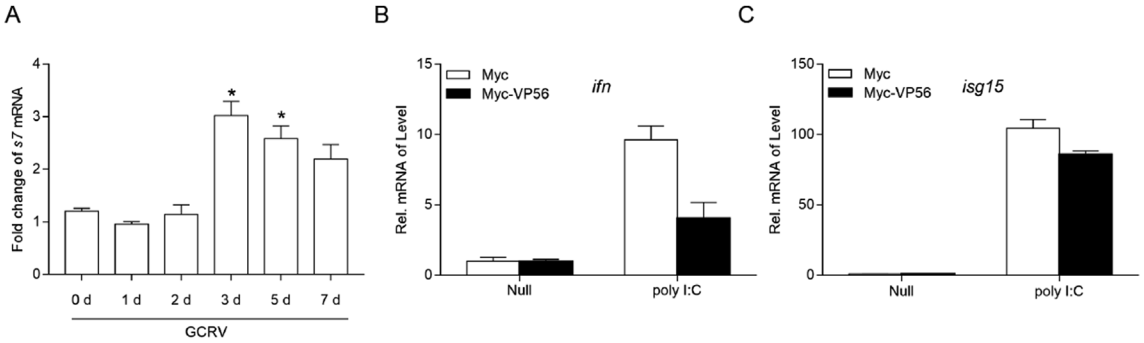

Fig. 1. VP56 is stimulated by virus infection. . (A) qPCR detection of the transcriptional levels of s7 on stimulation. GCO cells were seeded on 6-well plates overnight and infected with GCRV (100 μl of the filtered virus-containing supernatant of frozen and thawed GCO cells, which was diluted 100 times with PBS) At the time points 0, 1, 2, 3, 5 and 7 day, total RNA was extracted for further qPCR assays.(B and C) VP56 inhibits poly I:C-induced IFN expression. GCO cells seeded into 6-well plates overnight were transfected with 2 μg Myc-VP56 or the empty vector and transfected with poly I:C (2 μg/ml) at 24 h post-transfection. At 24 h post transfection, total RNAs were extracted to examine the transcriptional levels of cellular *ifn* and *isg15* by qPCR. The relative transcription levels were normalized to the transcription level of the *β-actin* gene and are represented as fold induction relative to the transcription level in control cells, which was set to 1. Data were expressed as mean ± SEM, $n = 3$. Asterisks indicate significant differences from control (*, $p < 0.05$). All experiments were repeated for at least three times with similar result.

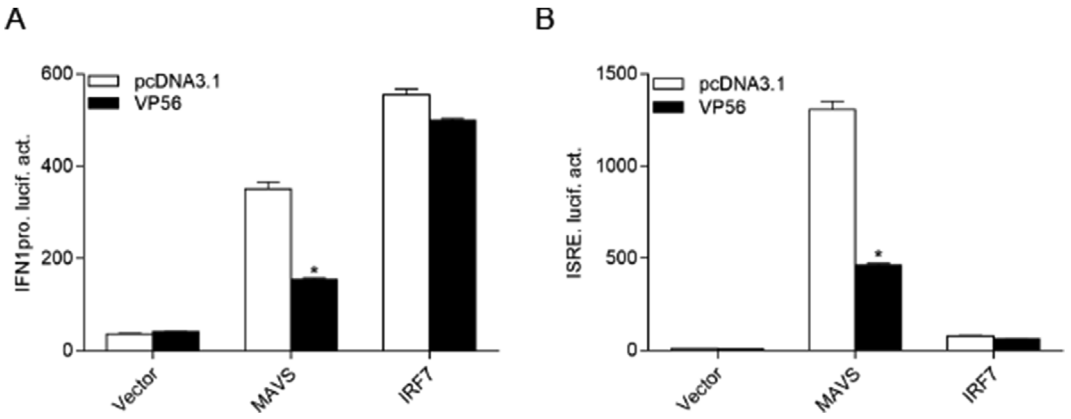

Fig. 2. VP56 inhibits MAVS-mediated IFN1 activation. (A and B) EPC cells were seeded on 24-well plates overnight and co-transfected with MAVS, IRF7, and pcDNA3.1-VP56 or pcDNA3.1 (+) plus IFN1pro (A) or ISRE-Luc (B) at the ratio of 1:1:1 (0.5 μg for each). pRL-TK was used as a control. At 24 h post transfection, cells were collected for detection of luciferase activities. The promoter activity is presented as relative light units normalized to Renilla luciferase activity. Data were expressed as mean ± SEM, $n = 3$. Asterisks indicate significant differences from control (*, $p < 0.05$). All experiments were repeated for at least three times with similar result.

increased significantly in GCO cells, which indicated that the cells were successfully infected with GCRV (Fig. 1A). Four type I IFNs (IFN1-IFN4) have been identified in grass carp, but only IFN1 can be significantly activated by poly I:C, a mimic of viral RNA [35] (data not shown). Thus, grass carp IFN1 was used in this study. As shown in Fig. 1B, poly I:C stimulation induced the upregulation of IFN1 transcripts; however, such induction was significantly impeded by the overexpression of VP56. Moreover, VP56 also blocked the poly I:C-activated expression of *isg15* (Fig. 1C). These data indicate that GCRV VP56 serves as a negative regulator to interfere with host IFN production.

3.2. VP56 suppresses IFN1 activation mediated by MAVS

Fish RLR factors are efficient for triggering IFN production [14]. Consequently, grass carp RLR constructs and IFN1 promoter (IFN1pro) were employed in the following studies. As shown in Fig. 2A, the overexpression of MAVS and IRF7 upregulated the activation of IFN1pro, and the activation of IFN1pro induced by MAVS was inhibited by co-transfection with VP56. However, the ectopic expression of VP56 did not affect the IRF7-stimulated IFN1pro activity. In the host IFN response, the ISRE motif is considered the binding site of ISGs that responds to transcriptional factors. After co-transfection with VP56 and ISRE-Luc and RLR factors, the upregulation of ISRE activity activated by MAVS but not IRF7 was reduced by VP56 (Fig. 2B). Collectively, these results suggest that VP56 decreases IFN production via negatively regulating MAVS.

3.3. VP56 associates with the RLR axis and locates in the cytoplasm

To further explore the function of VP56, whether VP56 interacts with RLRs at the protein level was investigated. HEK 293T cells were co-transfected with Myc-VP56 and Flag-tagged RLR factors, including MAVS, TBK1, MITA, IRF3, and IRF7. The results showed that most of the anti-Flag Ab-immunoprecipitated protein complexes were recognized by the anti-Myc Ab, which suggests that VP56 associates with TBK1, MITA, IRF3, and IRF7 but not MAVS (Fig. 3A). Next, the subcellular location of VP56 was monitored in EPC cells. Confocal microscopy revealed that the VP56-EGFP signal was mainly distributed in the cytoplasm (Fig. 3B). We co-transfected DsRed-MAVS, DsRed-MITA, DsRed-TBK1, DsRed-IRF3, or DsRed- IRF7 with VP56-EGFP. A red signal from TBK1, IRF3, and IRF7 was observed in the cytosol and almost overlapped with the green signal from VP56 (Fig. 3C–G). Taken together, these data suggest that VP56 is located in the cytosol and associates with RLR factors.

3.4. VP56 decreases the TBK1-mediated phosphorylation of IRF7

To investigate the regulatory mechanism of VP56 on the RLR axis, we examined the effect of VP56 on RLR molecules at the protein level. MAVS-, TBK1-, MITA-, IRF3-, and IRF7-HA expression vectors were co-transfected with Myc-VP56 or an empty vector. As shown in Fig. 4A, overexpressed VP56 did not cause any obvious change in RLR molecules at the protein level. Given that IRF3/7 phosphorylation is indispensable for mediating the IFN response, whether the phosphorylation of IRF3/7 is influenced by VP56 needs to be clarified. First, the function of grass carp TBK1 was investigated. As shown in Fig. 4B and C, both IRF3 and IRF7 caused a band shift and exhibited higher mobilities when they were co-transfected with TBK1-Flag in 293T cells. Subsequently, the cell lysates were incubated with CIP. As expected, the band shifts disappeared, demonstrating that IRF3 and IRF7 are also phosphorylated by TBK1 in grass carp. Then, we evaluated whether IRF3/7 phosphorylation would be impaired by the overexpression of VP56. As shown in Fig. 4D and E, the amount of IRF7 was dramatically reduced by the overexpression of VP56 in a dose-dependent manner; in contrast, VP56 had minimal effects on the IRF3 level. Similar results occur in zebrafish (Fig. 4F and G). These results suggest that VP56 specifically promotes the degradation of IRF7.

3.5. VP56 triggers the K48-linked ubiquitination and degradation of IRF7

Protein degradation is one of the main strategies involved in modulating protein functions in biological processes and there are two main systems for protein degradation: ubiquitin proteasome and autophagosome pathways. To identify the degradation pathway of IRF7, the cells were treated with indicated inhibitors. The VP56-mediated degradation of IRF7 was completely inhibited by the proteasome inhibitor MG132 but not 3-MA, which is an autophagosome pathway inhibitor (Fig. 5A). Since ubiquitination is an important process during proteasome-dependent degradation, we further determined whether the degradation of IRF7 was due to ubiquitination. HEK 293T cells were transfected with Flag-TBK1, Myc-IRF7, HA-VP56, and HA-Ub in the presence or absence of MG132. Following the immunoprecipitation of Myc-IRF7, IB revealed that VP56 potentiated the ubiquitination of IRF7 (Fig. 5B). K48 and K63, the lysines at positions 48 and 63 of ubiquitin linked with polyubiquitin chains, are two canonical polyubiquitin chain linkages. Given that K48-linked polyubiquitin chain modification leads to the targeting of proteins for proteasome recognition and degradation, whereas K63-linked polyubiquitin chain modification enhances the stability of target proteins [36–38], we chose to investigate whether

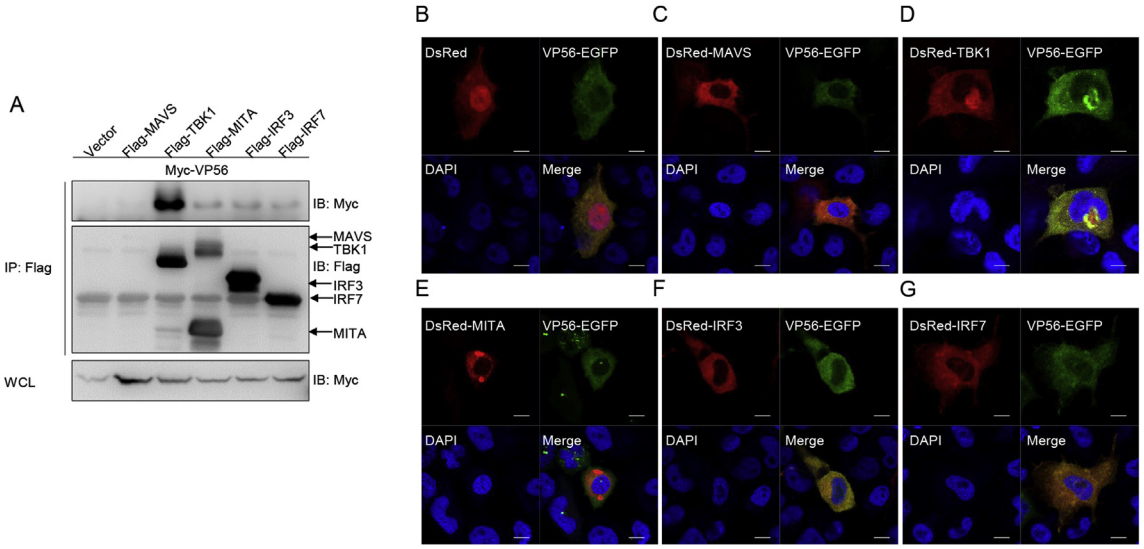

Fig. 3. VP56 locates in the cytoplasm and interacts with the RLRs. (A) HEK 293T cells seeded into 10-cm^2 dishes were transfected with empty vector or Flag-MAVS/TBK1/MITA/IRF3/IRF7 and Myc-VP56 (5 μg each). After 24 h, cell lysates were IP with anti-Flag affinity gel. The immunoprecipitates and WCLs were then analyzed by IB with anti-Flag and anti-Myc Abs, respectively. (B) EPC cells seeded on microscopy cover glass in 6-well plates were transfected with 2 μg of VP56-EGFP and 2 μg of empty vector or DsRed-MAVS/TBK1/MITA/IRF3/IRF7. After 24 h, the cells were fixed and subjected to confocal microscopy analysis. Green signals represent overexpressed VP56 protein, red signals represent overexpressed MAVS, TBK1, MITA, IRF3, or IRF7, and blue staining indicates the nucleus region (a × 63 oil immersion objective). Scale bar, 10 μm. All experiments were repeated at least three times with similar results. (For interpretation of the references to colour in this figure legend, the reader is referred to the Web version of this article.)

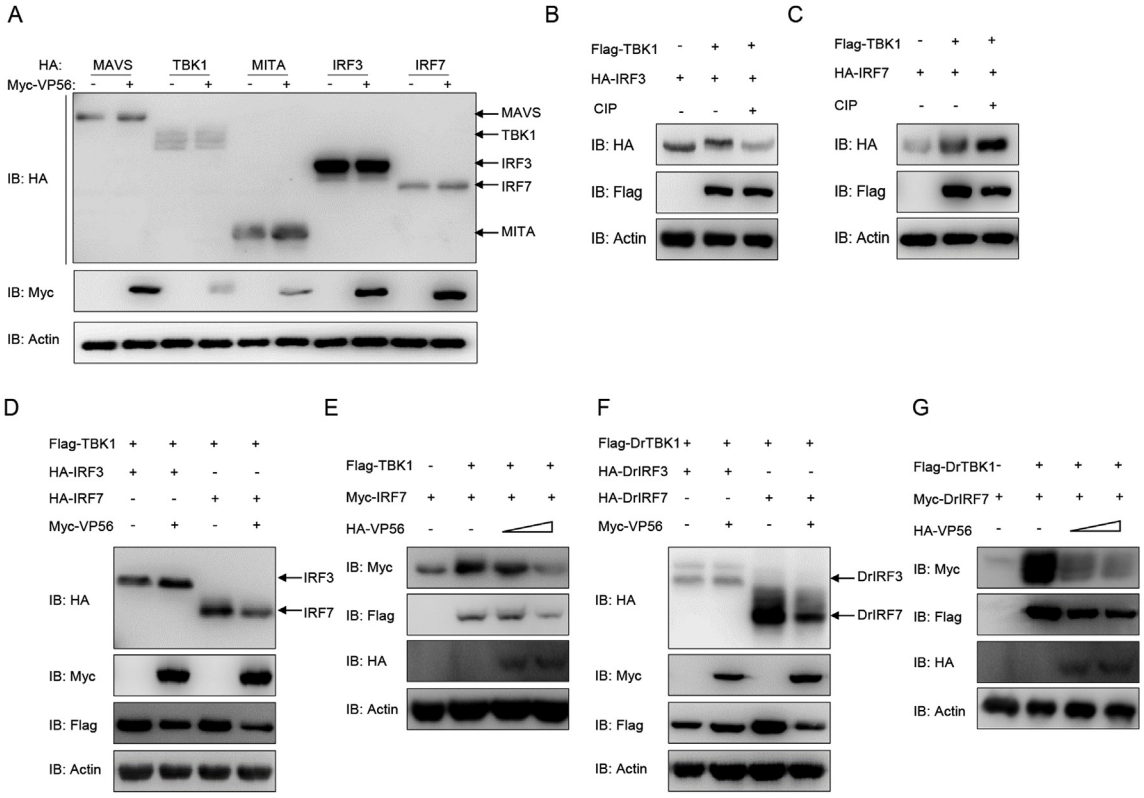

Fig. 4. VP56 decreases the phosphorylation of IRF7 mediated by TBK1. (A) VP56 has no significant effect on RLR protein expression. HEK 293T cells were seeded in 6-well plates overnight and transfected with 2 μg of HA-RLRs and 2 μg of empty vector or Myc-VP56 for 24 h. The WCLs were subjected to IB with the anti-HA, anti-Myc, and anti-β-actin Abs. (B and C) TBK1 mediates the phosphorylation of IRF3 and IRF7. HEK 293T cells were seeded into 6-well plates overnight and transfected with Flag-TBK1 and HA-IRF3/IRF7 (2 μg for each) for 24 h. The cell lysates (100 μg) were treated with or without CIP (10 U) for 40 min at 37 °C. The lysates were then detected by IB with anti-HA, anti-Flag and anti-β-actin Abs. (D and F) HEK 293T cells were seeded into 6-well plates overnight and co-transfected with 1 μg Flag-TBK1 or Flag-DrTBK1 plus 1 μg empty vector or HA-VP56, together with 1 μg Myc-IRF7 or Myc-DrIRF7 for 24 h. The lysates were then subjected to IB with anti-Myc, anti-Flag, anti-HA, and anti-β-actin Abs. (E and G)HEK 293T cells were seeded into 6-well plates overnight and co-transfected with 1 μg Flag-TBK1 or Flag-DrTBK1 plus various concentration of HA-VP56 (0.5 μg, or 1 μg, or 2 μg, empty vector was used to make up the rest), together with 1 μg Myc-IRF7 or Myc-DrIRF7 for 24 h. The lysates were then subjected to IB with anti-Myc, anti-Flag, anti-HA and anti-β-actin Abs. All experiments were repeated at least three times with similar results.

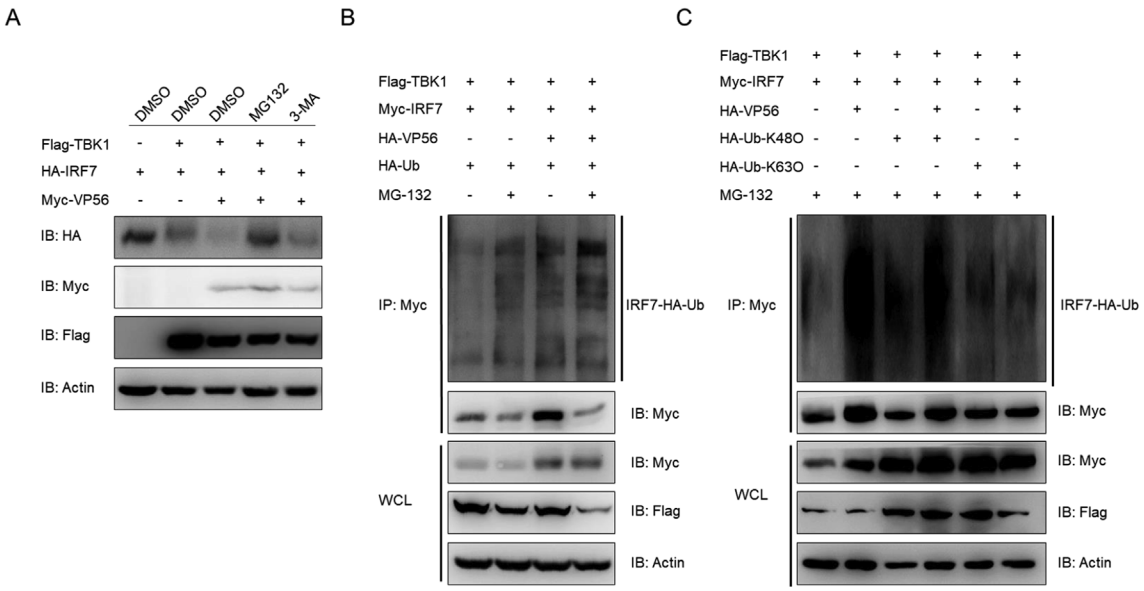

Fig. 5. VP56 promotes K48-linked ubiquitination and degradation of IRF7. (A) HEK 293T cells were seeded in 6-well plates overnight and transfected with 1 μg HA-IRF7 and 1 μg empty vector, or Myc-VP56 and 1 μg Flag-TBK1. At 18 h post-transfection, the cells were treated with the indicated inhibitors for 6 h prior to being harvested for IB analysis of WCLs with the anti-HA, anti-Myc, anti-Flag, and anti-β-actin Abs. (B) EPC cells were seeded in 10-cm^2 dishes and transfected with 4 μg Flag-TBK1, 4 μg Myc-IRF7, 4 μg HA-VP56 or empty vector, and 2 μg HA-Ub. At 18 h post transfection, the cells were treated with DMSO or MG132 for 6 h. Cell lysates were IP with anti-Myc-affinity gels. Then the immunoprecipitates and WCLs were analyzed by IB with the Abs indicated. (C) EPC cells were seeded in 10-cm^2 dishes and transfected with 4 μg Flag-TBK1, 4 μg Myc-IRF7, 4 μg HA-VP56 or empty vector, and 2 μg HA-Ub-K48O or HA-Ub-K63O. At 18 h post-transfection, the cells were treated with MG132 for 6 h. Cell lysates were IP with anti-Myc-affinity gels. Then the immunoprecipitates and WCLs were analyzed by IB with the indicated Abs. All experiments were repeated for at least three times with similar results.

VP56 promoted the K48- or K63-linked ubiquitination of IRF7. To achieve this goal, plasmids expressing ubiquitin mutants and retaining only a single lysine residue either K48 (ubiquitin-K48) or K63 (ubiquitin-K63) were used. As shown in Fig. 5C, immunoprecipitation and IB indicated that VP56 promoted IRF7 ubiquitination with wild-type ubiquitin and ubiquitin-K48 but not with ubiquitin-K63. The above results indicate that VP56 induces the K48-linked ubiquitination of IRF7, which is recognized and subsequently degraded by the proteasome pathway.

3.6. VP56 attenuates the cellular IFN response and facilitates SVCV replication

To determine whether VP56 interferes with the cellular IFN response to facilitate virus proliferation, EPC cells were transfected with VP56 or the empty vector and infected with SVCV. Total RNAs were extracted and monitored by qPCR. As shown in Fig. 6A and B, the expression of the *ifn* transcript in the cells that overexpress VP56 was reduced compared to their levels in the control cells and the reduced expression of host *vig1* was also observed. Moreover, more CPE was observed in the VP56 group at 2 d post-infection (Fig. 6C). This was confirmed by the titer of SVCV, which had significantly increased (5,800-fold) in the VP56-overexpressing cells compared to the control cells (Fig. 6D). These data demonstrate that VP56 suppresses the cellular IFN response and enhances the capacity of SVCV to replicate.

4. Discussion

As in mammals, fish IFN plays a critical role in the host immune response when defending against viral infection. However, aquatic viruses still cause high mortality in the cultured fish industries. The immune evasion mechanisms involved in the pathogenesis of aquatic viruses remain poorly understood. Here, we report that GCRV VP56 interacts with IRF7 and promotes the K48-linked ubiquitination and degradation of IRF7, which suppresses the host IFN response.

GCRV, the first viral pathogen identified from aquatic animals in China in 1983, causes a serious epidemic of hemorrhagic disease, which results in extremely high mortality among grass carp [1]. The GCRV virion consists of 11 dsRNA genome segments surrounded by multiple concentric protein capsids [8]. The 11 segments encode seven structural proteins and five nonstructural proteins. Five of these proteins (VP1-VP4 and VP6) form the core layer [39]. The functional exploration of non-structural proteins among the 11 segments remains unclear. We have reported that VP41 prevents the fish IFN response by attenuating the phosphorylation of MITA for viral evasion [40]. Further study in this manuscript has revealed that VP56 interacts with IRF7 and promotes the ubiquitination and degradation of IRF7. Many viruses have evolved strategies to elude the host immune system and one or several host immune molecules may be involved in this evasion because of viruses' relatively limited genome capacity [41].

RLRs toll-like receptor (TLR)- and NOD-like receptor (NLR)-mediated immune responses are the first line of defense against pathogenic microbes [12]. The IFN system is a particularly critical component in the host response, including the induction of IFN, IFN-mediated signaling, and the amplification of the IFN response [42]. IRF7 is a critical component of the intrinsic immune system [43]. Although various PRRs activate different signal pathways, most signals transduction ultimately converge on IRF7. In addition, IRF7 is induced by viral infection and is essential for sustained transcriptional activation of IFN genes [44]. In response to host defend mechanisms, viruses have evolved various strategies to inhibit the activation of IRF7, including inhibiting IRF7 dimerization and altering IRF7 modification (sumoylation, phosphorylation, or ubiquitination) [45–48]. In fish, antiviral effects of IRF7 has been reported in crucian carp, zebrafish, and grass carp [49,50]. Following GCRV infection, host induces a series of antiviral immune responses, then stimulates the transcription of a broad range of ISGs including *irf7*, which in turn establish an antiviral state within the cells to eliminate viral infection [51]. However, viruses have established multiple mechanisms to counteract host antiviral state [52]. So far, the relationships between fish viruses and IRF7 are not well known. In the

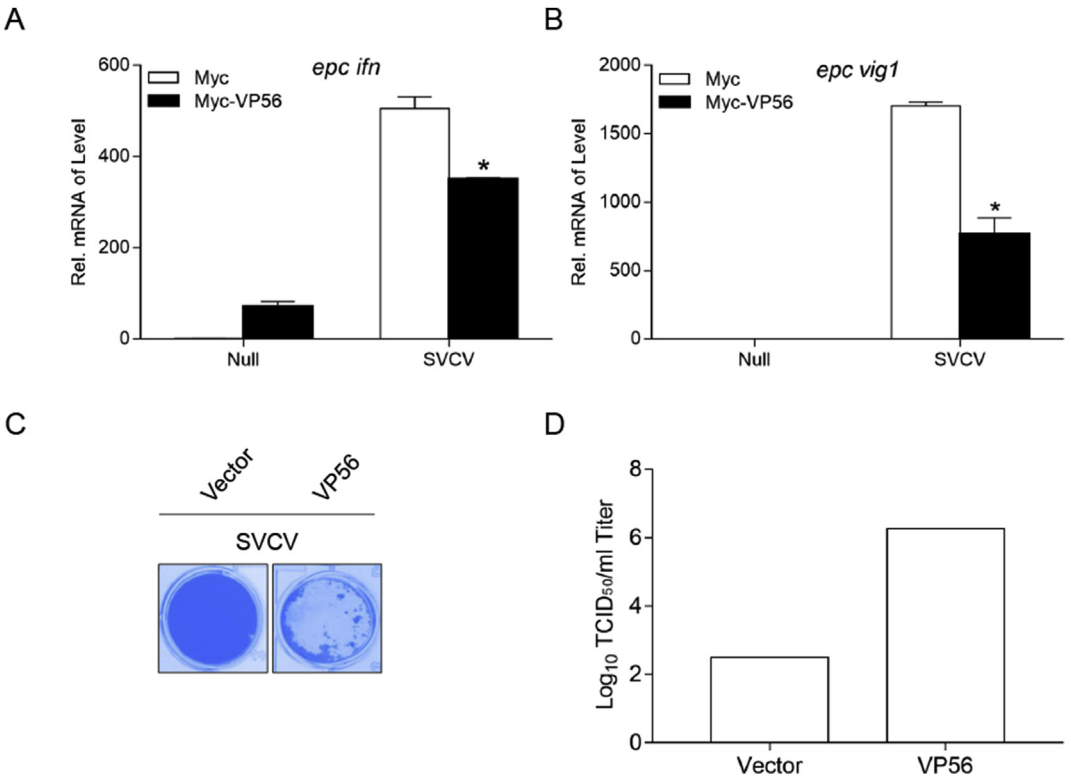

Fig. 6. VP56 dampens the cellular IFN response and facilitates SVCV proliferation. (A and B) EPC cells seeded into 6-well plates overnight were infected with SVCV (MOI = 1). After 24 h, total RNAs were extracted to examine the transcriptional levels of cellular *epcifn* and *epcvig1* by qPCR. The relative transcription levels were normalized to the transcription level of the β-actin gene and are represented as fold induction relative to the transcription level in control cells, which was set to 1. Data were expressed as mean ± SEM, $n = 3$. Asterisks indicate significant differences from control (*, $p < 0.05$). (C and D) EPC cells seeded in 24-well plates overnight were transfected with 0.5 μg pcDNA3.1 (+)-VP56 or pcDNA3.1 (+) vector. At 24 h post-transfection, cells were infected with SVCV (MOI = 0.001) for 48 h. (C) Then, cells were fixed with 4% PFA and stained with 1% crystal violet. (D) Culture supernatants from the cells infected with SVCV were collected, and the viral titer was measured by standard $TCID_{50}$ method. All experiments were repeated for at least three times with similar results. (For interpretation of the references to colour in this figure legend, the reader is referred to the Web version of this article.)

present study, GCRV VP56 induced the degradation of IRF7, resulting in the reduction of IFN expression. These results demonstrate that fish virus also possesses the function to antagonize host IFN response.

Ubiquitination, which is a reversible covalent modification, plays an important role in regulating the stability, activity, and localization of target proteins [53]. Many viruses have taken advantage of ubiquitination to target host proteins and change the proteins' original state in immune signaling pathways. For example, the N-terminal protease fragment (NPro) of the Bovine viral diarrhea virus (BVDV) blocks the binding of IRF3 to DNA and targets IRF3 for proteasomal degradation, thus blocking IFN production [54]; Severe acute respiratory syndrome coronavirus (SARS-CoV) papain-like protease (PLPro) inhibits the TLR7-mediated IFN induction by removing the polyubiquitination of TRAF3 and TRAF6 [55]; the N protein of SVCV suppresses fish IFNϕ1 expression by degrading MAVS in an ubiquitination-proteasome manner [34]. Here, our results reveal that GCRV VP56 represses IFN production by inducing the K48-linked ubiquitination and degradation of IRF7.

In conclusion, the current study reveals a potential vital mechanism used by VP56 of GCRV to negatively regulate IRF7 through the ubiquitination-proteasome degradation pathway. These data shed light on the novel manner of immune evasion utilized by GCRV. Further studies are needed to ascertain the functions of other proteins of GCRV in immune evasion, which will promote an in-depth understanding of GCRV pathogenesis and provide ideas for preventive strategies.

Funding

This work was supported by the National Natural Science Foundation of China (31930114, 31725026) and the Science Fund for Creative Research Groups of the Natural Science Foundation of Hubei Province of China (2018CFA011) provided to Yong-An Zhang, as well as the National Key Research and Development Program of China (2018YFD0900504) and Youth Innovation Promotion Association provided to Shun Li.

Declaration of competing interest

We declare no financial and commercial conflicts of interest.

Acknowledgments

We thank Dr. Fang Zhou (Institute of Hydrobiology, Chinese Academy of Sciences) for assistance with confocal microscopy analysis and Dr. Feng Xiong (China Zebrafish Resource Center, Institute of Hydrobiology, Chinese Academy of Sciences) for RNA sample extraction.

Appendix A. Supplementary data

Supplementary data to this article can be found online at https://doi.org/10.1016/j.fsi.2020.02.004.

References

[1] A.A.C. Rangel, D.D. Rockemann, F.M. Hetrick, S.K. Samal, Identification of grass carp haemorrhage virus as a new genogroup of aquareovirus, J. Gen. Virol. 80 (1999) 2399–2402.

[2] Q. Wang, W. Zeng, C. Liu, C. Zhang, Y. Wang, C. Shi, S. Wu, Complete genome sequence of a reovirus isolated from grass carp, indicating different genotypes of GCRV in China, J. Virol. 86 (22) (2012) 12466.

[3] Y. Yang, Z.Q. Peng, H. Li, S.W. Tan, H.Y. Yu, H. Yu, Epidemiological survey of grass carp (Ctenopharyngodon idella) reovirus in south China, and genetic variations of VP6 gene, Isr. J. Aquacult. Bamidgeh 69 (2017).

[4] L.P. Cheng, Q. Fang, S. Shah, I.C. Atanasov, Z.H. Zhou, Subnanometer-resolution structures of the grass carp reovirus core and virion, J. Mol. Biol. 382 (1) (2008) 213–222.

[5] H. Attoui, Q. Fang, F. Mohd Jaafar, J.F. Cantaloube, P. Biagini, P. de Micco, X. de Lamballerie, Common evolutionary origin of aquareoviruses and orthoreoviruses revealed by genome characterization of Golden shiner reovirus, Grass carp reovirus, Striped bass reovirus and golden ide reovirus (genus Aquareovirus, family Reoviridae), J. Gen. Virol. 83 (Pt 8) (2002) 1941–1951.

[6] F. Yu, L. Wang, W. Li, L. Lu, Identification of a novel membrane-associated protein from the S7 segment of grass carp reovirus, J. Gen. Virol. 100 (3) (2019) 369–379.

[7] Y.Y. Tian, Z.Z. Jiao, J.J. Dong, C.F. Sun, X.Y. Jiang, X. Ye, Grass carp reovirus-GD108 fiber protein is involved in cell attachment, Virus Gene. 53 (4) (2017) 613–622.

[8] C. Pei, F. Ke, Z.Y. Chen, Q.Y. Zhang, Complete genome sequence and comparative analysis of grass carp reovirus strain 109 (GCReV-109) with other grass carp reovirus strains reveals no significant correlation with regional distribution, Arch. Virol. 159 (9) (2014) 2435–2440.

[9] D. Xu, L. Song, H. Wang, X.Y. Xu, T. Wang, L.Q. Lu, Proteomic analysis of cellular protein expression profiles in response to grass carp reovirus infection, Fish Shellfish Immunol. 44 (2) (2015) 515–524.

[10] L.M. Peng, C.R. Yang, J.G. Su, Protective roles of grass carp Ctenopharyngodon idella Mx isoforms against grass carp reovirus, PloS One 7 (12) (2012).

[11] B. Wang, Y.B. Zhang, T.K. Liu, J. Shi, F. Sun, J.F. Gui, Fish viperin exerts a conserved antiviral function through RLR-triggered IFN signaling pathway, Dev. Comp. Immunol. 47 (1) (2014) 140–149.

[12] S. Akira, S. Uematsu, O. Takeuchi, Pathogen recognition and innate immunity, Cell 124 (4) (2006) 783–801.

[13] F. Sun, Y.B. Zhang, J. Jiang, B. Wang, C. Chen, J. Zhang, J.F. Gui, Gig 1, a novel antiviral effector involved in fish interferon response, Virology 448 (2014) 322–332.

[14] T. Kawai, S. Akira, Innate immune recognition of viral infection, Nat. Immunol. 7 (2) (2006) 131–137.

[15] O. Takeuchi, S. Akira, Recognition of viruses by innate immunity, Immunol. Rev. 220 (2007) 214–224.

[16] T.H. Mogensen, Pathogen recognition and inflammatory signaling in innate immune defenses, Clin. Microbiol. Rev. 22 (2) (2009) 240-+.

[17] R.B. Seth, L.J. Sun, C.K. Ea, Z.J.J. Chen, Identification and characterization of MAVS, a mitochondrial antiviral signaling protein that activates NF-kappa B and IRF3, Cell 122 (5) (2005) 669–682.

[18] L.G. Xu, Y.Y. Wang, K.J. Han, L.Y. Li, Z.H. Zhai, H.B. Shu, VISA is an adapter protein required for virus-triggered IFN-beta signaling, Mol. Cell. 19 (6) (2005) 727–740.

[19] T. Kawai, K. Takahashi, S. Sato, C. Coban, H. Kumar, H. Kato, K.J. Ishii, O. Takeuchi, S. Akira, IPS-1, an adaptor triggering RIG-I- and Mda5-mediated type I interferon induction, Nat. Immunol. 6 (10) (2005) 981–988.

[20] E. Meylan, J. Curran, K. Hofmann, D. Moradpour, M. Binder, R. Bartenschlager, R. Tschopp, Cardif is an adaptor protein in the RIG-I antiviral pathway and is targeted by hepatitis C virus, Nature 437 (7062) (2005) 1167–1172.

[21] K.A. Fitzgerald, S.M. McWhirter, K.L. Faia, D.C. Rowe, E. Latz, D.T. Golenbock, A.J. Coyle, S.M. Liao, T. Maniatis, IKKepsilon and TBK1 are essential components of the IRF3 signaling pathway, Nat. Immunol. 4 (5) (2003) 491–496.

[22] M. Sato, H. Suemori, N. Hata, M. Asagiri, K. Ogasawara, K. Nakao, T. Nakaya, M. Katsuki, S. Noguchi, N. Tanaka, T. Taniguchi, Distinct and essential roles of transcription factors IRF-3 and IRF-7 in response to viruses for IFN-alpha/beta gene induction, Immunity 13 (4) (2000) 539–548.

[23] K. Honda, A. Takaoka, T. Taniguchi, Type I interferon [corrected] gene induction by the interferon regulatory factor family of transcription factors, Immunity 25 (3) (2006) 349–360.

[24] S. Biacchesi, M. LeBerre, A. Lamoureux, Y. Louise, E. Lauret, P. Boudinot, M. Bremont, Mitochondrial antiviral signaling protein plays a major role in induction of the fish innate immune response against RNA and DNA viruses, J. Virol. 83 (16) (2009) 7815–7827.

[25] S. Biacchesi, E. Merour, A. Lamoureux, J. Bernard, M. Bremont, Both STING and MAVS fish orthologs contribute to the induction of interferon mediated by RIG-I, PloS One 7 (10) (2012) e47737.

[26] N. Yu, X. Xu, G. Qi, D. Liu, X. Chen, X. Ran, Z. Jiang, Y. Li, H. Mao, C. Hu, Ctenopharyngodon idella TBK1 activates innate immune response via IRF7, Fish Shellfish Immunol. 80 (2018) 521–527.

[27] H. Feng, Q.M. Zhang, Y.B. Zhang, Z. Li, J. Zhang, Y.W. Xiong, M. Wu, J.F. Gui, Zebrafish IRF1, IRF3, and IRF7 differentially regulate IFN Phi 1 and IFN Phi 3 expression through assembly of homo- or heteroprotein complexes, J. Immunol. 197 (5) (2016) 1893–1904.

[28] B. Huang, W.S. Huang, P. Nie, Cloning and expression analyses of interferon regulatory factor (IRF) 3 and 7 genes in European eel, Anguilla anguilla with the identification of genes involved in IFN production, Fish Shellfish Immunol. 37 (2) (2014) 239–247.

[29] T.H. Kim, H.J. Zhou, Functional Analysis of Chicken IRF7 in Response to dsRNA Analog Poly(I:C) by Integrating Overexpression and Knockdown (vol 10, e0133450, 2015), PloS One 10 (9) (2015).

[30] K. Liu, G. Ma, X. Liu, Y. Lu, S. Xi, A. Ou, J. Wei, B. Li, D. Shao, Y. Li, Y. Qiu, D. Miao, Z. Ma, Porcine reproductive and respiratory syndrome virus counteracts type I interferon-induced early antiviral state by interfering IRF7 activity, Vet. Microbiol. 229 (2019) 28–38.

[31] Q. Xue, H. Liu, Z. Zhu, F. Yang, L. Ma, X. Cai, Q. Xue, H. Zheng, Seneca Valley Virus 3C(pro) abrogates the IRF3- and IRF7-mediated innate immune response by degrading IRF3 and IRF7, Virology 518 (2018) 1–7.

[32] S.W. Hwang, D. Kim, J.U. Jung, H.R. Lee, KSHV-encoded viral interferon regulatory factor 4 (vIRF4) interacts with IRF7 and inhibits interferon alpha production, Biochem. Bioph. Res. Co. 486 (3) (2017) 700–705.

[33] L.F. Lu, S. Li, Z.X. Wang, S.B. Liu, D.D. Chen, Y.A. Zhang, Zebrafish NDRG1a negatively regulates IFN induction by promoting the degradation of IRF7, J. Immunol. 202 (1) (2019) 119–130.

[34] L.F. Lu, S. Li, X.B. Lu, S.E. LaPatra, N. Zhang, X.J. Zhang, D.D. Chen, P. Nie, Y.A. Zhang, Spring viremia of carp virus N protein suppresses fish IFNphi1 production by targeting the mitochondrial antiviral signaling protein, J. Immunol. 196 (9) (2016) 3744–3753.

[35] Z. Liao, Q. Wan, J. Su, Bioinformatics analysis of organizational and expressional characterizations of the IFNs, IRFs and CRFBs in grass carp Ctenopharyngodon idella, Dev. Comp. Immunol. 61 (2016) 97–106.

[36] B. Zhong, L. Zhang, C.Q. Lei, Y. Li, A.P. Mao, Y. Yang, Y.Y. Wang, X.L. Zhang, H.B. Shu, The ubiquitin ligase RNF5 regulates antiviral responses by mediating degradation of the adaptor protein MITA, Immunity 30 (3) (2009) 397–407.

[37] T. Tsuchida, J.A. Zou, T. Saitoh, H. Kumar, T. Abe, Y. Matsuura, T. Kawai, S. Akira, The ubiquitin ligase TRIM56 regulates innate immune responses to intracellular double-stranded DNA, Immunity 33 (5) (2010) 765–776.

[38] J.S. Ye, N. Kim, K.J. Lee, Y.R. Nam, U. Lee, C.H. Joo, Lysine 63-linked TANK-binding kinase 1 ubiquitination by mindbomb E3 ubiquitin protein ligase 2 is mediated by the mitochondrial antiviral signaling protein, J. Virol. 88 (21) (2014) 12765–12776.

[39] X. Ye, Y.Y. Tian, G.C. Deng, Y.Y. Chi, X.Y. Jiang, Complete genomic sequence of a reovirus isolated from grass carp in China, Virus Res. 163 (1) (2012) 275–283.

[40] L.F. Lu, S. Li, Z.X. Wang, S.Q. Du, D.D. Chen, P. Nie, Y.A. Zhang, Grass carp reovirus VP41 targets fish MITA to abrogate the interferon response, J. Virol. 91 (14) (2017).

[41] J.Y. Min, R.M. Krug, The primary function of RNA binding by the influenza A virus NS1 protein in infected cells: inhibiting the 2 '-5 ' oligo (A) synthetase/RNase L pathway, Proc. Natl. Acad. Sci. U.S.A. 103 (18) (2006) 7100–7105.

[42] J.E. Durbin, A. Fernandez-Sesma, C.K. Lee, T.D. Rao, A.B. Frey, T.M. Moran, S. Vukmanovic, A. Garcia-Sastre, D.E. Levy, Type I IFN modulates innate and specific antiviral immunity, J. Immunol. 164 (8) (2000) 4220–4228.

[43] S. Ning, J.S. Pagano, G.N. Barber, IRF7: activation, regulation, modification and function, Gene Immun. 12 (6) (2011) 399–414.

[44] K. Honda, H. Yanai, H. Negishi, M. Asagiri, M. Sato, T. Mizutani, N. Shimada, Y. Ohba, A. Takaoka, N. Yoshida, T. Taniguchi, IRF-7 is the master regulator of type-I interferon-dependent immune responses, Nature 434 (7034) (2005) 772–777.

[45] T. Kubota, M. Matsuoka, T.H. Chang, P. Tailor, T. Sasaki, M. Tashiro, A. Kato, K. Ozato, Virus infection triggers SUMOylation of IRF3 and IRF7, leading to the negative regulation of type I interferon gene expression, J. Biol. Chem. 283 (37) (2008) 25660–25670.

[46] L. Unterholzner, R.P. Sumner, M. Baran, H.W. Ren, D.S. Mansur, N.M. Bourke, F. Randow, G.L. Smith, A.G. Bowie, Vaccinia virus protein C6 is a virulence factor that binds TBK-1 adaptor proteins and inhibits activation of IRF3 and IRF7, PLoS Pathog. 7 (9) (2011).

[47] S.W. Hwang, D. Kim, J.U. Jung, H.R. Lee, KSHV-encoded viral interferon regulatory factor 4 (vIRF4) interacts with IRF7 and inhibits interferon alpha production, Bio.chem. Bioph. Res. Co. 486 (3) (2017) 700–705.

[48] Y. Kitagawa, M. Yamaguchi, M. Zhou, M. Nishio, M. Itoh, B. Gotoh, Human parainfluenza virus type 2 V protein inhibits TRAF6-mediated ubiquitination of IRF7 to prevent TLR7-and TLR9-dependent interferon induction, J. Virol. 87 (14) (2013) 7966–7976.

[49] D. Li, W. Tan, M. Ma, X. Yu, Q. Lai, Z. Wu, G. Lin, C. Hu, Molecular characterization and transcription regulation analysis of type I IFN gene in grass carp (Ctenopharyngodon idella), Gene 504 (1) (2012) 31–40.

[50] L.F. Lu, S. Li, X.B. Lu, Y.A. Zhang, Functions of the two zebrafish MAVS variants are opposite in the induction of IFN1 by targeting IRF7, Fish Shellfish Immunol. 45 (2) (2015) 574–582.

[51] Q. Wan, C. Yang, Y. Rao, Z. Liao, J. Su, MDA5 induces a stronger interferon response than RIG-I to GCRV infection through a mechanism involving the phosphorylation and dimerization of IRF3 and IRF7 in CIK cells, Front. Immunol. 8 (2017) 189.

[52] A. Garcia-Sastre, C.A. Biron, Type 1 interferons and the virus-host relationship: a lesson in detente, Science 312 (5775) (2006) 879–882.

[53] V.G. Bhoj, Z.J. Chen, Ubiquitylation in innate and adaptive immunity, Nature 458 (7237) (2009) 430–437.

[54] L. Hilton, K. Moganeradj, G. Zhang, Y.H. Chen, R.E. Randall, J.W. McCauley, S. Goodbourn, The NPro product of bovine viral diarrhea virus inhibits DNA binding by interferon regulatory factor 3 and targets it for proteasomal degradation, J. Virol. 80 (23) (2006) 11723–11732.

[55] S.W. Li, C.Y. Wang, Y.J. Jou, S.H. Huang, L.H. Hsiao, L. Wan, Y.J. Lin, S.H. Kung, C.W. Lin, SARS coronavirus papain-like protease inhibits the TLR7 signaling pathway through removing lys63-linked polyubiquitination of TRAF3 and TRAF6, Int. J. Mol. Sci. 17 (5) (2016).